

# Simulation of an AmBe source and Helium-3 Thermal Neutron Detectors

Using GEANT4

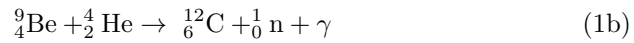
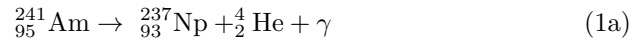
Samuel de Jong  
Department of Physics and Astronomy  
University of Victoria

August 30, 2017

## 1 Introduction

### 1.1 AmBe neutron source

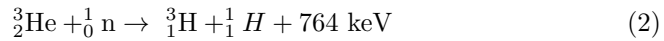
The University of Victoria has a  $^{241}\text{Am}$  neutron source, which produces neutrons using the following reaction [3]:



with an activity of 168 GBq (measured at 185 GBq in 1966). The energy spectrum of an AmBe source can be found in Fig 1. The configuration of the University of Victoria's AmBe source can be found in [4]. The neutron rates from five different AmBe sources is measured in [5]. From this, it is determined that an AmBe source produces  $6.08 \pm 0.17 \times 10^4$  neutrons/GBq. For the 168 GBq source, this corresponds to  $1.02 \pm 0.03 \times 10^7$  neutrons/s.

### 1.2 Helium-3 Tube

When a thermal neutron (with an energy of 0.025 eV) passes through the active area of the detector, it may be captured by a  $^3\text{He}$  atom [1]:



The cross section for this reaction decreases as the energy of the neutron increases, as shown in Fig 3. The  $^3\text{H}$  and proton ionize the gas in the tubes. This ionization produces a signal on a sense wire in the centre of the tube.

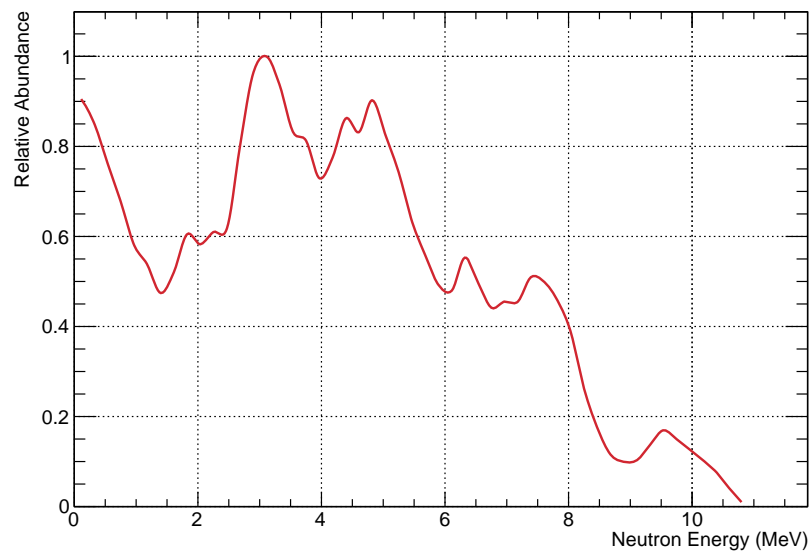


Figure 1: Energy spectrum of neutrons from AmBe source [2].



Figure 2: Helium-3 tube

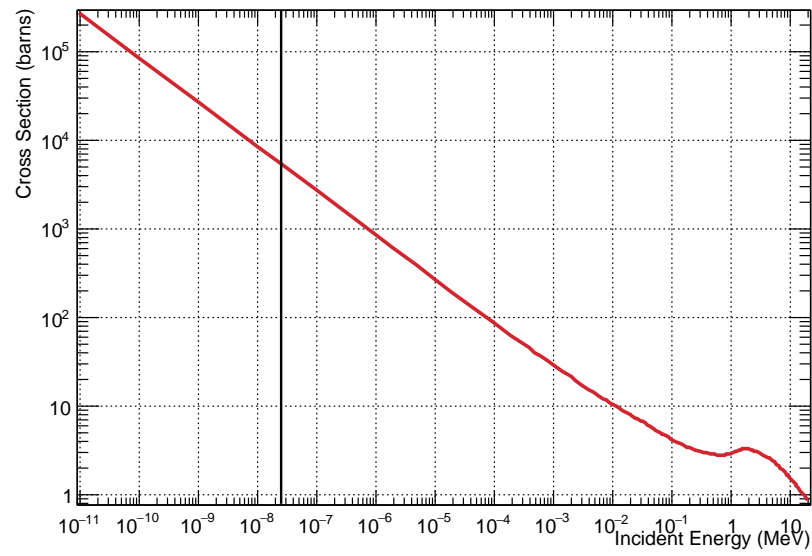


Figure 3: Cross section of neutron capture by helium-3 as a function of neutron energy. The vertical black line corresponds to upper range of the energy of thermal neutrons [6].

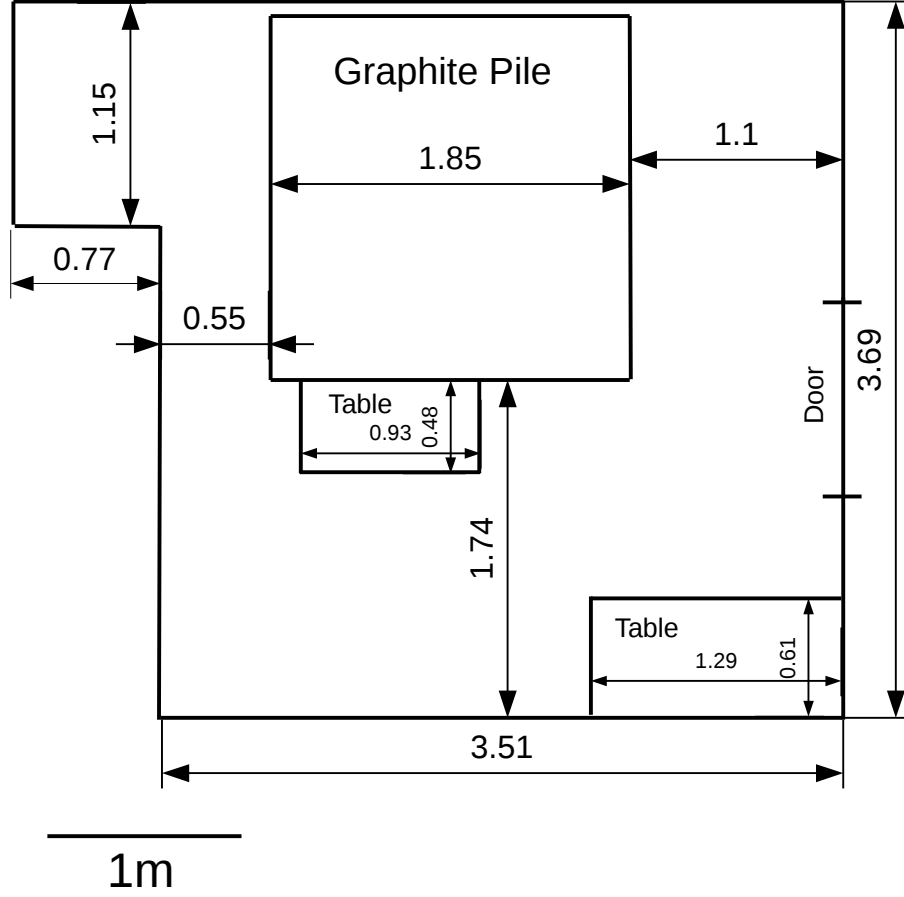


Figure 4: Scale drawing of the pile room

## 2 Geometry

The centre of the geometry is defined to be the centre of the graphite cube. All other positions are taken relative to this point. The geometry of the pile room is read into the simulation from four files:

**Room.xml** contains geometry of the room. The dimensions of the room, the material the walls are composed of, the thickness of the walls, and the position of the centre of the room relative to the graphite are all contained in this file. The default dimensions are taken from fig 4, the default material is G4\_CONCRETE, GEANT4's implementation of concrete, and the thickness is assumed to be 20 cm. The door to the room and the small alcove on the left of fig 4 have been omitted from the room description.

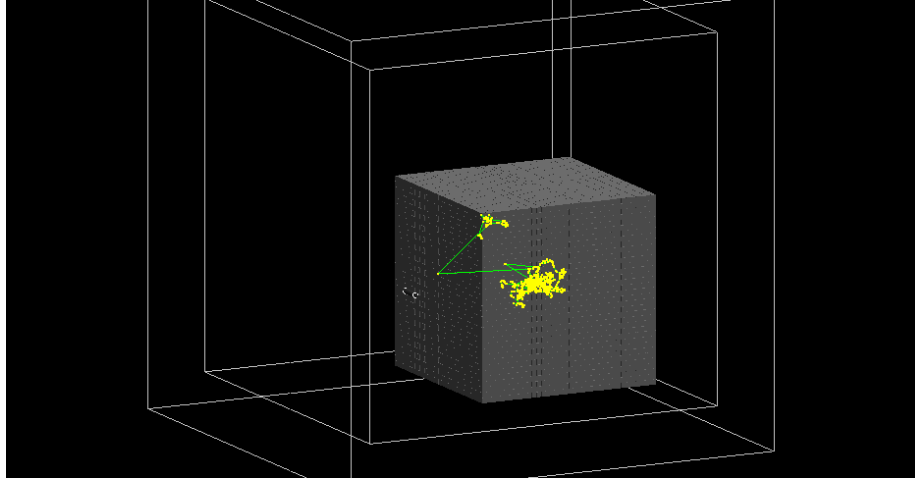


Figure 5: Geometry as implemented in GEANT4. Yellow lines indicate the trajectory of a neutron event.



Figure 6: Photograph of the graphite pile showing rods

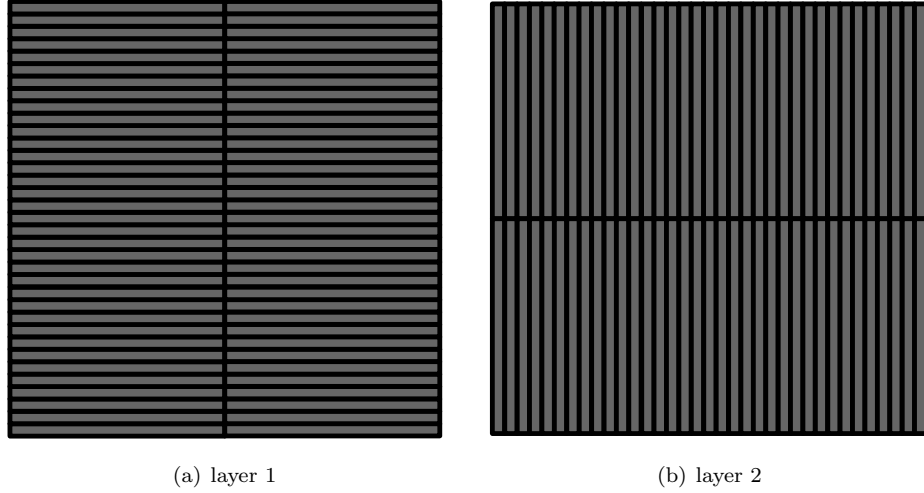


Figure 7: Arrangement of rods in alternating layers

**Graphite.xml** contains the geometry of the graphite. The graphite pile is composed of layers of criss-crossed rods of graphite, as shown in fig 6.

For simplicity, only the dimensions of one rod are defined in the xml file, as well as the number of layers in the pile. The default length of a rod is 92.5 cm with width of 5.285 cm. Each layer is two rods long and 35 wide, as shown in fig 7, with each layer rotated  $90^\circ$  with respect to the previous. The pile is composed of 35 layers. The length and width of each rod is reduced by a Gaussian distributed random number in order to simulate the imperfect stacking and variation in rod dimensions of the actual pile.

The material of the pile is G4.GRAPHITE with a small boron impurity. The density and the purity of the graphite (in %) are specified in the xml file.

**HE3TUBE.xml** contains the geometry of the helium-3 tubes. The dimensions of the tubes are based on fig 8. The xml file can contain several tubes, each of which is implemented in the simulation.

**misc.xml** contains the geometry of any other object, such as a polyethylene shield. Both boxes and cylinders can be implemented. The position of the object can be with respect to the origin (the centre of the graphite) or with respect to one of the helium-3 tubes. The xml file can contain several objects, all of which will be implemented in the simulation.

### 3 Output Ntuples

A root file containing two ntuples is produced by the simulation:

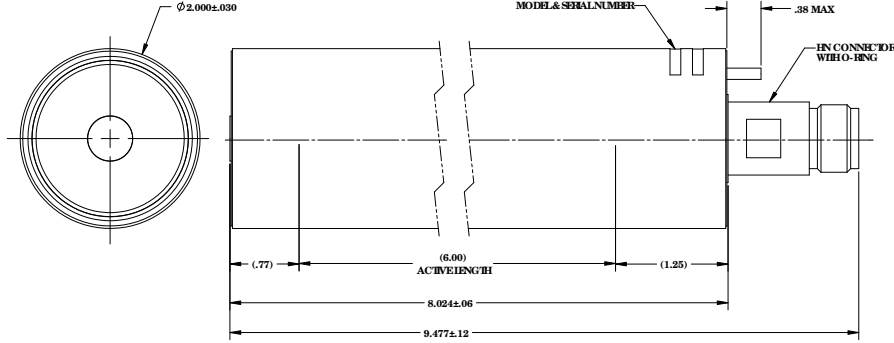


Figure 8: Schematic of helium-3 tube

Branch	Description
Ekin_n_PostGraphite	Kinetic energy of a neutron after leaving the graphite
Etot_n_initial	Initial energy of neutron
TotalEnergyDeposited	Total energy deposited by a proton and tritium
leftWall	1 if the neutron left the wall of the room
he3TubeXPos	X position of tube containing a neutron hit
he3TubeYPos	Y position of tube containing a neutron hit
he3TubeZPos	Z position of tube containing a neutron hit
EDEPinHe3	a vector of the energy deposits in the helium-3 tubes
PIDinHe3	a vector of the PID of particles causing energy deposits in the helium-3 tubes
neutronHits	The channel number of a tube where a hit occurred
diffusionRadius	a vector containing 100 radius values between 30 and 70 cm
diffusionFlux	a vector containing the number of neutrons which cross a sphere defined by each entry in diffusionRadius

Table 1: Branches in the PileRoomSim ntuple

**geometry** contains the geometry of the room, graphite cube, helium-3 tubes, and the miscellaneous objects. This ntuple has only one entry. The values are taken from the xml files used in the simulation.

**PileRoomSim** contains the simulation results. By default, only events containing a neutron hit in a helium-3 tube are saved, but it is possible to save all events. The branches in this ntuple summarized in table 1

## 4 Determination of Boron Contamination

Why??

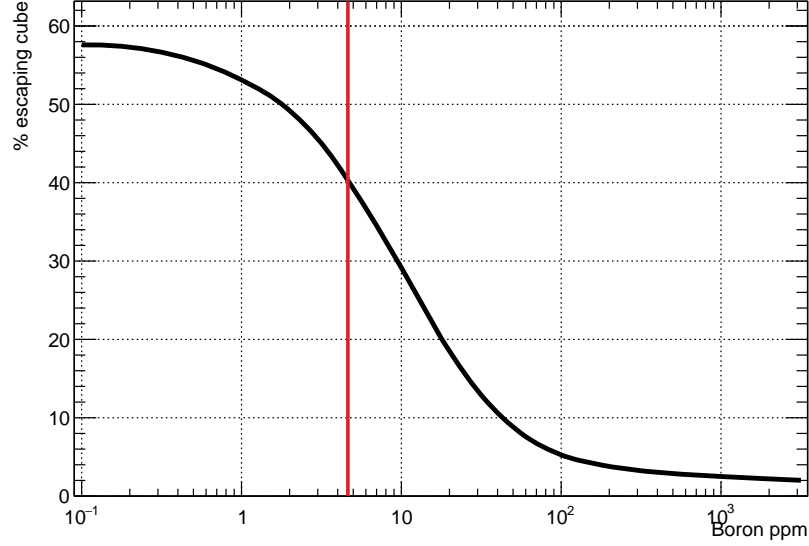


Figure 9: Fraction of neutrons which escape the graphite as a function of boron ppm

#### 4.1 Diffusion length approach

In the winter of 2017, an undergraduate student at UVic performed an experiment which measured the diffusion length of thermal neutrons in the graphite of the neutron source. The result of this experiment was a diffusion length of  $(0.429 \pm 0.008)$  m [7]. The accepted value for the diffusion length on graphite is 0.503 m. I hypothesized that the difference between the measured value and the accepted value was due to a small boron impurity on the graphite.

I performed a measurement of the diffusion length in the simulated graphite pile. The diffusion length is related to the neutron flux by this relationship:

$$\phi = A \cdot \exp(-\gamma r) \quad (3a)$$

$$\gamma^2 = 1/L^2 \quad (3b)$$

Where  $\phi$  is the neutron flux,  $r$  is the distance from the source, and  $L$  is the diffusion length.

In the simulation the number of neutrons which enter or exit a shell of radius  $r$  was counted, then divided by the surface area of the shell to get the neutron flux:

$$\phi = \frac{N_{\text{neutrons}}}{4\pi r^2} \quad (4)$$

This was plotted against the distance from the source (see fig 10) was then fit



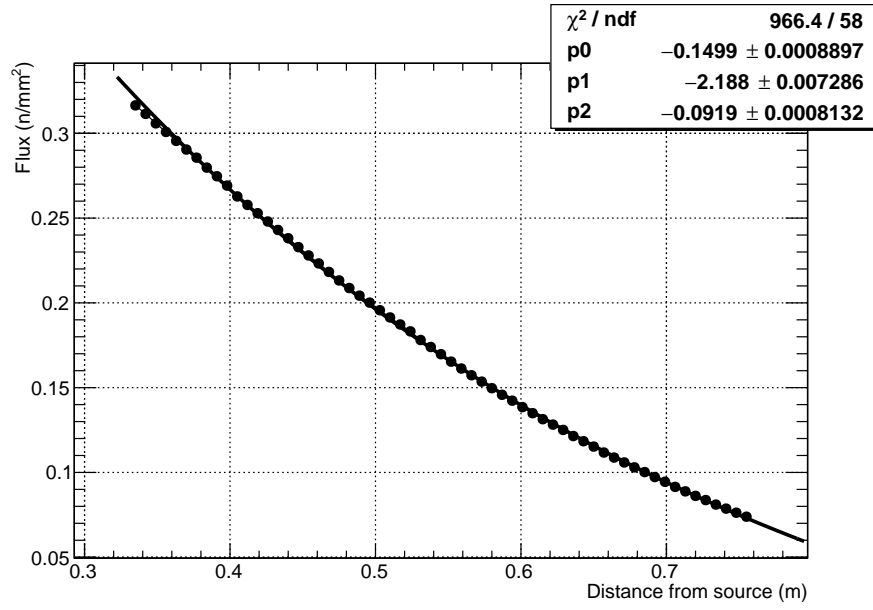


Figure 10: Neutron flux as a function of distance from the source for pure graphite

to

$$\phi = p_0 \cdot \exp(p_1 r) + p_2 \quad (5)$$

so that  $L = 1/p_1$ . The range of  $r$  was chosen so that a diffusion length of 0.503 m would be produced by pure graphite.

This process was repeated with boron impurities added (see fig 11). The boron contamination which produced a diffusion length of 0.429 m was  $4.63 \times 10^{-4}\%$  or 4.63 ppm boron.

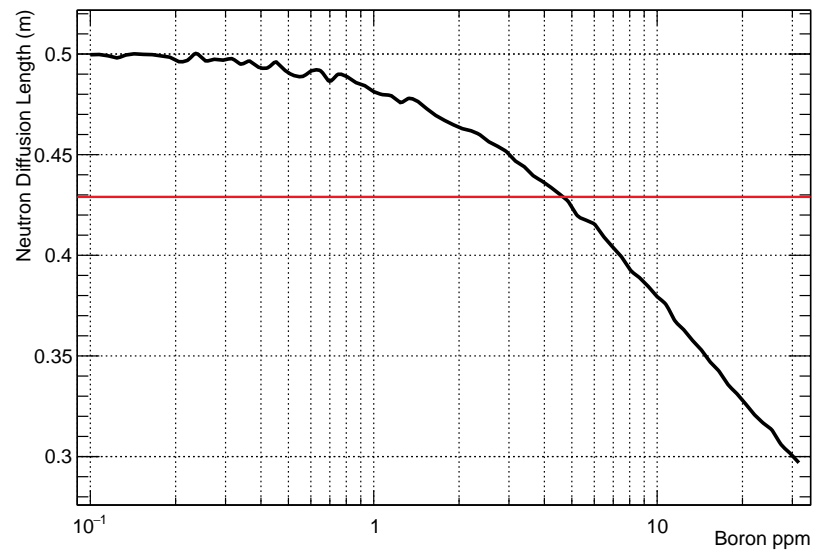


Figure 11: Neutron diffusion length as a function of boron contamination. The red line indicates the value of the diffusion length from the undergraduate experiment.

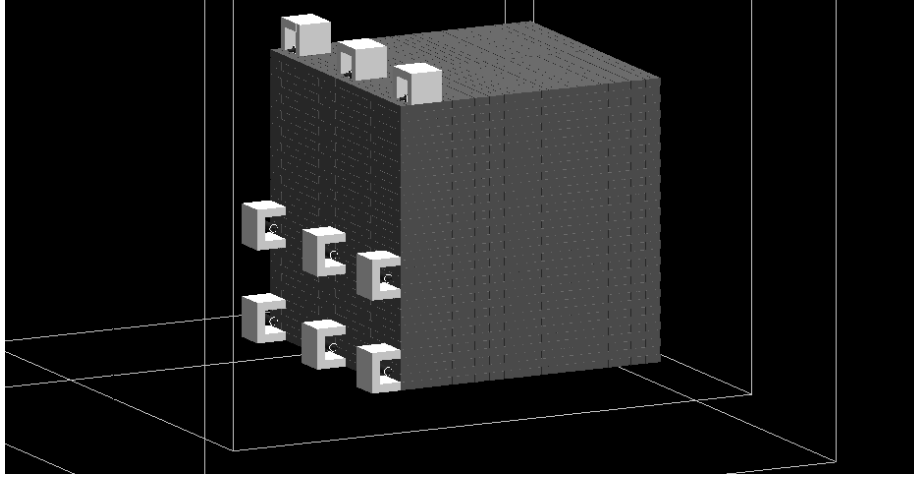


Figure 12: Locations of measurement on the face of the graphite. The white rectangles are polyethylene blocks to reduce the rate of neutrons from the walls.

## 4.2 Face measurement approach

An alternative approach to determining the concentration of boron impurities was to measure the rate at different positions on the face of the graphite cube and compare with the simulated rate at the same positions. The positions measured and simulated can be seen in fig 12. The helium-3 tubes were surrounded with blocks of polyethylene to reduce the rate of neutrons bouncing back from the walls of the room.

I noticed that the number of neutrons detected in each helium-3 tube was related to the number of neutrons which escape the graphite. This is shown in fig 13. Each vertical set of data points is from a simulation sample with a different boron contamination. For each of the positions shown in fig 12, a least squares fit to a linear function was performed.

Shown in fig 14 is the neutron escape rate vs boron contamination. Using the fits from fig 13, I was able to calculate how many neutrons would be measured at each position for boron concentrations from  $10^{-5}\%$  -  $10^{-2.5}\%$ . The ratio of the rate in at each position to the rate at the centre position was taken for data and for simulation. For each boron concentration, a  $\chi^2$  value was calculated for the difference in between data and simulation:

$$\chi^2 = \sum_{p=1, p \neq 5}^{p=9} \left[ \left( \left. \frac{R_p}{R_5} \right|_{\text{Data}} - \left. \frac{R_p}{R_5} \right|_{\text{Sim}} \right)^2 / \left( \left. \frac{R_p}{R_5} \right|_{\text{Data}} \right) \right] \quad (6)$$

This is shown in fig 15. The minimum  $\chi^2$  is at a boron concentration of 0.00221% or 22.1 ppm, which is approximately five times the predicted concentration from the diffusion approach.

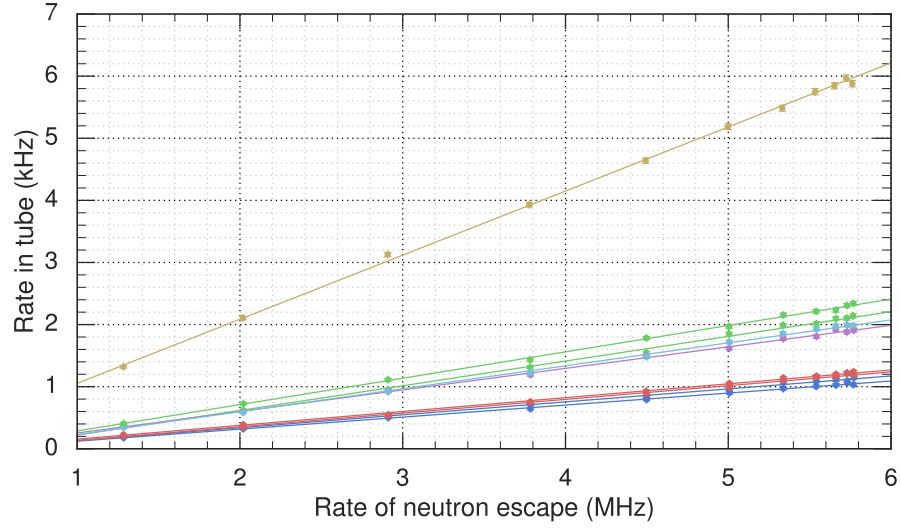


Figure 13: Helium-3 tube rate vs neutron escape rate for the nine different positions shown in fig 12, with linear fit.

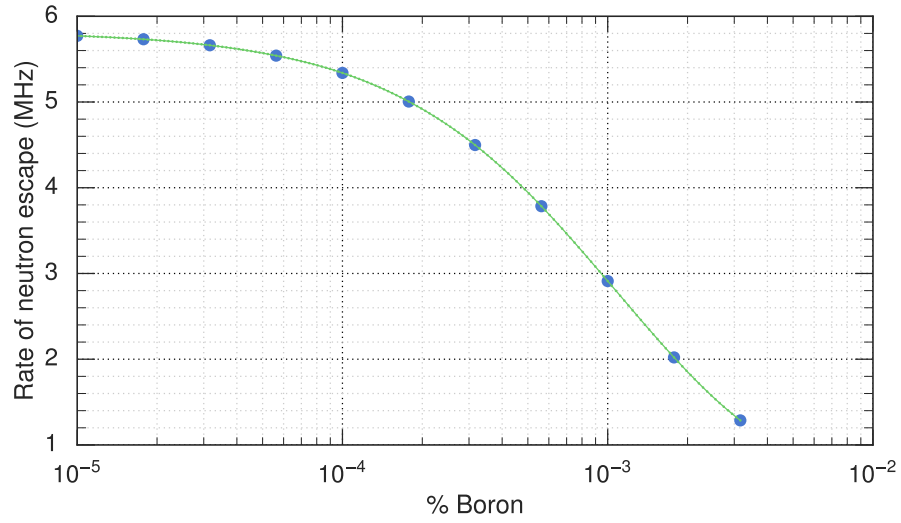


Figure 14: Neutron escape rate vs boron concentration. Blue are from full simulation, green are interpolated points.

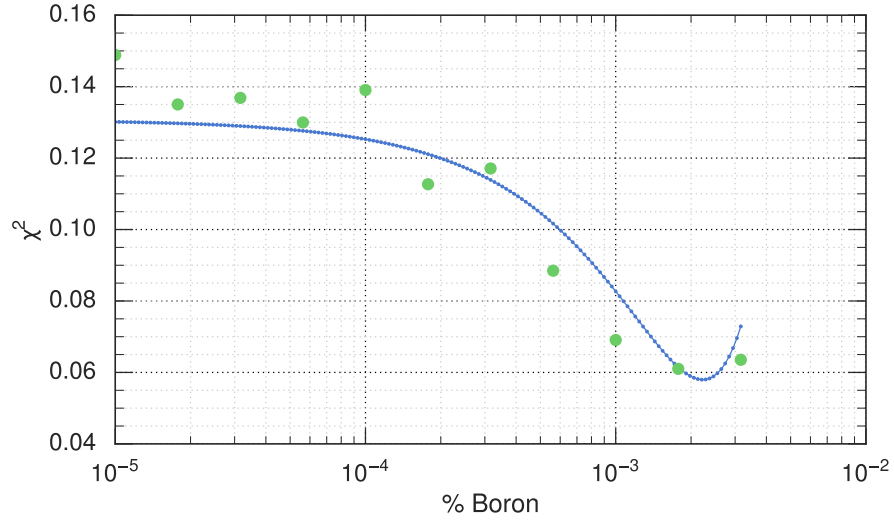


Figure 15:  $\chi^2$  of comparison between data and simulation vs boron concentration. The green points are from full simulation, blue is using the extrapolation technique described here.

## 5 TODO

GEANT4 mixes by mass  
determine boron contamination in natural graphite  
which boron % to use

## References

- [1] Oed A. Detectors for thermal neutrons. *Nuclear Instruments and Methods in Physics Research Section A: Accelerators, Spectrometers, Detectors and Associated Equipment*, 525(12):62 – 68, 2004. Proceedings of the International Conference on Imaging Techniques in Subatomic Physics, Astrophysics, Medicine, Biology and Industry.
- [2] Kluge H and Weise K. The neutron energy spectrum of a  $^{241}\text{Am}$ -Be ( $\alpha$ , n) source and resulting mean fluence to dose equivalent conversion factors. *Radiation Protection Dosimetry*, 2(2):85–93, 1982.
- [3] Barschall HH. *Neutron sources: for basic physics and applications*, volume 2. Pergamon, 1983.
- [4] Geiger KW and Hargrove CK. Neutron spectrum of an  $\text{Am}^{241}$ -Be ( $\alpha$ , n) source. *Nuclear Physics*, 53:204–208, 1964.
- [5] Lebreton L, Zimbal A, and Thomas D. Experimental comparison of  $^{241}\text{Am}$ -Be neutron fluence energy distributions. *Radiation protection dosimetry*, 2007.
- [6] Brookhaven National Laboratory. Evaluated nuclear data file. <http://www.nndc.bnl.gov>, December 2011.
- [7] Deanna Pineau. Thermal diffusion of neutrons in graphite. *UVic undergraduate lab report*, 2017.